


ARTICLE

<https://doi.org/10.1038/s42003-019-0385-7>

OPEN

Structural and biochemical analyses of the nuclear pore complex component ELYS identify residues responsible for nucleosome binding

Wataru Kobayashi^{1,2}, Yoshimasa Takizawa¹, Maya Aihara², Lumi Negishi¹, Hajime Ishii² & Hitoshi Kurumizaka ^{1,2}

The nuclear pore complex embedded within the nuclear envelope is the essential architecture for trafficking macromolecules, such as proteins and RNAs, between the cytoplasm and nucleus. The nuclear pore complex assembly occurs on chromatin in the post-mitotic phase of the cell cycle. ELYS (MEL-28/AHCTF1) binds to the nucleosome, which is the basic chromatin unit, and promotes assembly of the complex around the chromosomes in cells. Here we show that the Arg-Arg-Lys (RRK) stretch of the C-terminal ELYS region plays an essential role in the nucleosome binding. The cryo-EM structure and the crosslinking mass spectrometry reveal that the ELYS C-terminal region directly binds to the acidic patch of the nucleosome. These results provide mechanistic insight into the ELYS-nucleosome interaction, which promotes the post-mitotic nuclear pore complex formation around chromosomes in cells.

¹Laboratory of Chromatin Structure and Function, Institute for Quantitative Biosciences, The University of Tokyo, 1-1-1 Yayoi, Bunkyo-ku, Tokyo 113-0032, Japan. ²Graduate School of Advanced Science and Engineering, Waseda University, 2-2 Wakamatsu-cho, Shinjuku-ku, Tokyo 162-8480, Japan. Correspondence and requests for materials should be addressed to H.K. (email: kurumizaka@iam.u-tokyo.ac.jp)

In eukaryotes, genomic DNA is organized into chromosomes and is accommodated within the nucleus. Histones are the major protein components of chromosomes and form the nucleosome as a basic unit¹. In the nucleosome, 145–147 base pairs of DNA segments are lefthandedly wrapped 1.65 turns around the histone octamer, composed of two each of histones H2A, H2B, H3, and H4^{2–4}. The nucleosomes are connected by short linker DNA segments and appear as chromatin with a beads-on-a-string configuration¹.

The chromosome conformation dynamically changes during the cell cycle^{5,6}. In interphase cells, the chromosomes are diffused within the nucleus, which is encircled by the nuclear envelope^{5,6}. The nuclear pore complexes (NPCs) are embedded in the nuclear envelope, and materials, such as proteins and RNAs, are transported between the nucleus and cytoplasm through the NPCs^{7–9}. In higher eukaryotes, the NPCs are disassembled concomitant with the breakdown of the nuclear envelope in mitotic cells. The duplicated chromosomes are then segregated into the dividing cells^{10–12}. After the chromosome segregation, reassembly of the nuclear envelope and NPCs occurs at segregated chromosomes, and then the functional nucleus is established in the daughter cells^{10,11,13–15}.

A nucleoporin, ELYS, plays a key role in post-mitotic NPC assembly^{16–18}. ELYS localizes to the nuclear rim in interphase cells and recruits NPC components, such as the Nup107–160 sub-complex, to chromosomes^{16–18}. The ELYS-knockdown HeLa cells are severely defective in the NPC formation^{16–18}. Consistently, in *Caenorhabditis elegans*, the knockdown of the ELYS homologue, MEL-28, induces an NPC assembly deficiency^{19,20}. These findings suggested that ELYS functions as a primer for the post-mitotic NPC reassembly on chromosomes^{11,13,15–18,21}.

In agreement with the idea that ELYS mediates the NPC assembly on chromosomes, ELYS reportedly binds to chromatin with both the AT-hook DNA-binding domain^{18,22} and C-terminal region²³. ELYS directly binds to the histone H2A–H2B dimer and the nucleosome *in vitro*²³. Intriguingly, histone depletion in mouse zygotes or *Xenopus* egg extracts resulted in defective NPC assembly^{23,24}. These results suggest that the chromatin binding of ELYS is essential for the NPC assembly. However, the mechanistic details of the ELYS–nucleosome interaction have not been elucidated.

In the present study, we purified the ELYS C-terminal peptide containing the AT-hook DNA-binding domain and a conserved Arg–Arg–Lys (RRK) stretch. Biochemical analyses revealed that the ELYS C-terminal peptide efficiently binds to the nucleosome, and its RRK stretch, in addition to the AT-hook DNA-binding domain, may play an essential role for the nucleosome binding. Cryo-electron microscopy (cryo-EM) and crosslinking mass spectrometric analyses revealed that the ELYS C-terminal peptide binds to the acidic patches of the nucleosome surface. These presented data clarify how ELYS binds to the nucleosome.

Results

The RRK stretch of ELYS is important for nucleosome binding.

The *Xenopus laevis* ELYS protein is composed of 2408 amino acid residues, and its C-terminal region is reportedly involved in chromatin binding^{18,22–26}. The ELYS peptide containing amino acid residues 2281–2408 has been reported as a nucleosome binding fragment^{22,23}. We first purified the ELYS 2281–2408 peptide and found that the ELYS 2299–2408 fragment was somewhat resistant to trypsin proteolysis. We then prepared the C-terminal ELYS peptide containing amino acid residues 2299–2408 (named ELYS_C) (Fig. 1a and Supplementary Fig. 1a). The nucleosome was reconstituted with a 145 base-pair (bp) Widom 601 sequence, which does not appear in linker DNA

regions, thus eliminating possible interactions between ELYS_C and linker DNAs (Supplementary Fig. 1b). A gel filtration analysis revealed that ELYS_C stoichiometrically bound to the nucleosome (Fig. 1b). We then prepared ELYS_C as a glutathione S-transferase (GST)-fusion protein (Supplementary Fig. 1c) and performed the pull-down assay (Fig. 1c). ELYS_C contains the AT-hook DNA-binding domain, which reportedly binds to chromatin^{18,22,23,26}. The RRK stretch, composed of the Arg2404, Arg2405, and Lys2406 residues, exists near the C-terminal end (Fig. 1a). Consistent with the previous reports^{23,24}, the ELYS_C peptide efficiently bound to the nucleosome, and the AT-hook mutant (ELYS_C 2R-A), in which the ELYS Arg2332 and Arg2334 residues are replaced by Ala, drastically reduced its nucleosome binding, probably due to defective DNA binding (Fig. 1d, lanes 4 and 5). Interestingly, we found that the deletion of the C-terminal ten amino acid residues of ELYS_C (ELYS_C Δ10) abolished its nucleosome-binding ability (Fig. 1d, lane 6). This ELYS_C deletion mutant lacked the RRK stretch but retained the AT-hook domain, suggesting that the AT-hook residues may not bind histones. Therefore, the RRK stretch may primarily function in the nucleosome binding.

The ELYS basic residues are required for nucleosome binding.

To identify the ELYS_C amino acid residues responsible for the nucleosome binding, we performed a mutational analysis. The basic amino acid residues, such as Arg and Lys, potentially bind to the DNA backbone phosphates or the acidic patch of the nucleosome surface²⁷. The C-terminal 10 amino acid residues of ELYS include four basic amino acid residues, Arg2404, Arg2405, Lys2406, and Arg2408 (Fig. 2a). To determine whether these basic amino acid residues are involved in the nucleosome binding, we prepared the ELYS_C mutants, ELYS_C(R2404A), ELYS_C(R2405A), ELYS_C(K2406A), and ELYS_C(R2408A), in which the ELYS Arg2404, Arg2405, Lys2406, and Arg2408 residues were each replaced by Ala (Supplementary Fig. 1c). Interestingly, the amino acid substitution at each basic residue slightly decreased the nucleosome binding, but the effect was not substantial (Fig. 2b, lanes 6–9). In contrast, the nucleosome binding was almost abolished when the Arg2404, Arg2405, and Lys2406 residues of the RRK stretch were simultaneously replaced by Ala (Fig. 2b, lane 10). These results suggested that the RRK stretch is responsible for the nucleosome binding of ELYS.

The cryo-EM structure of the ELYS_C–nucleosome complex.

We performed a cryo-EM analysis of the ELYS_C–nucleosome complex. The nucleosome reconstituted with a 145 base-pair Widom 601 sequence was incubated with the GST-fused ELYS_C peptide, and the ELYS_C–nucleosome complex was fixed with paraformaldehyde and purified by the GraFix method. The cryo-EM images of the ELYS_C–nucleosome complexes were collected (Fig. 3a). The cryo-EM structure of the ELYS_C–nucleosome complex was reconstructed and refined to 4.3 Å resolution (Fig. 3b–d, Supplementary Fig. 2, and Table 1). In the structure, extra densities were clearly visible on the acidic patches of both surfaces of the nucleosome (Fig. 4a, b). These extra densities observed on the acidic patch may represent part of ELYS_C bound to the nucleosome. Although the shapes of these extra densities are slightly different, their density sizes are similar. Therefore, we suspected that these extra densities may be responsible for the same ELYS_C region.

Crosslinking mass spectrometric analysis. We performed a crosslinking mass spectrometric analysis. In this experiment, we used the crosslinker DSS-H12/D12, which mediates crosslinking between Lys residues. We found that the ELYS Lys2400 residue,

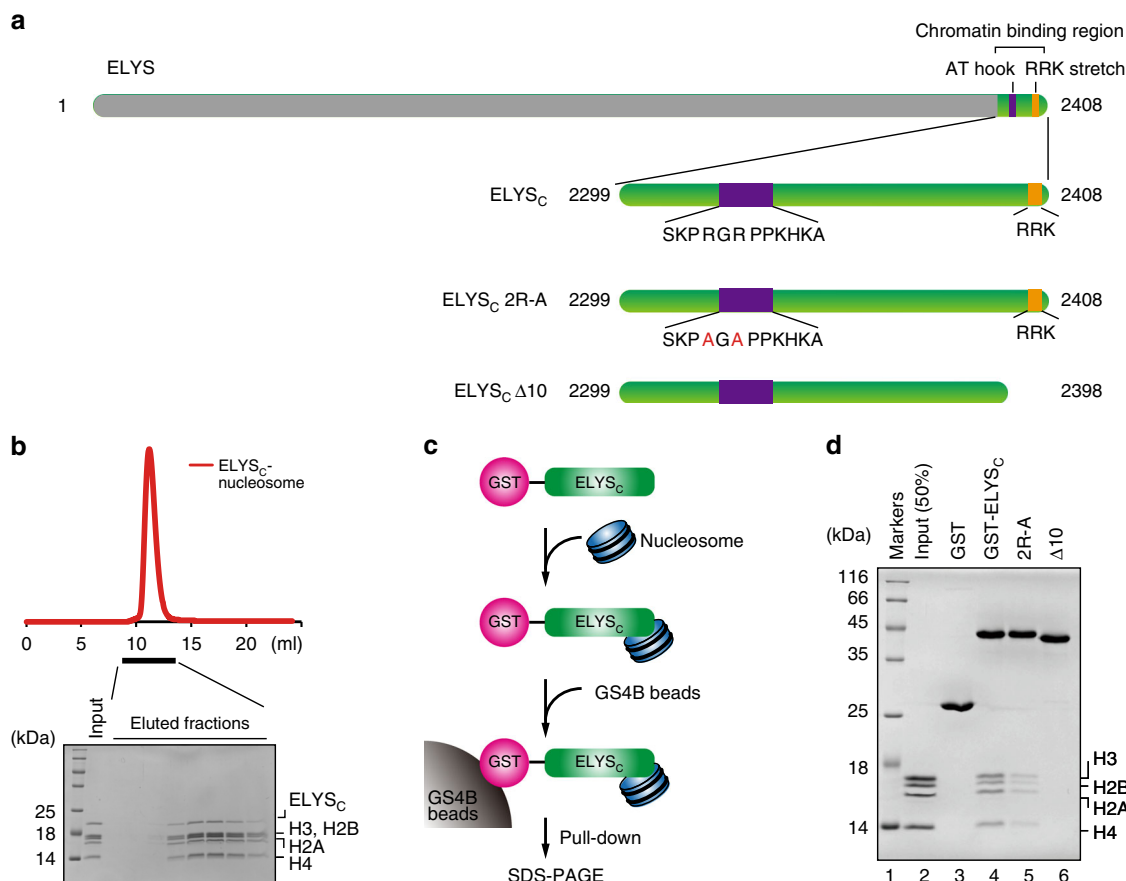


Fig. 1 Nucleosome binding by ELYS_C. **a** The *Xenopus laevis* ELYS_C fragments used in this study. The purple and orange boxes represent the regions corresponding to the AT-hook DNA-binding domain and the RRK stretch, respectively. In the ELYS_C 2R-A mutant, the Arg2332 and Arg2334 residues in the AT-hook DNA binding domain are replaced by Ala. The amino acid residues are numbered. In the ELYS_C Δ10 mutant, the C-terminal ten residues including the RRK stretch are deleted. The amino acid residues are numbered. **b** Gel-filtration analysis of the ELYS_C-nucleosome complex. ELYS_C and the nucleosome containing the 145 bp Widom 601 DNA were mixed in a 2.5:1 molar ratio, at room temperature for 20 min. The red line indicates the elution profile of the ELYS_C-nucleosome complex. Eluted fractions were analyzed by 18% sodium dodecyl sulfate-polyacrylamide gel electrophoresis (SDS-PAGE) with Coomassie Brilliant Blue staining. The uncropped gel image is shown in Supplementary Fig. 4. **c** Experimental scheme for the pull-down assay with GS4B beads. **d** The pull-down assay for the ELYS_C-nucleosome interaction. Lane 1 represents molecular mass markers. Lane 2 indicates input nucleosome (50%). Lane 3 indicates a negative control experiment with glutathione S-transferase (GST). Lanes 4–6 indicate the experiments with GST-ELYS_C, GST-ELYS_C 2R-A, and GST-ELYS_C Δ10. The samples were analyzed by 18% SDS-PAGE with Coomassie Brilliant Blue staining. Experiments were independently repeated four times, and consistent results were obtained. The uncropped gel image is shown in Supplementary Fig. 4

which is located near the RRK stretch, crosslinked with the H2A Lys95, H2B Lys120, and H3 Lys56 residues (Fig. 5a and Supplementary Fig. 3). These results indicated that the distances between the ELYS Lys2400 residue and the H2A Lys95, H2B Lys120, and H3 Lys56 residues are within 10–20 Å, because the crosslinking distance of DSS-H12/D12 is 10–20 Å²⁸. The ELYS Lys2406 residue in the RRK stretch was not detected as a cross-linked residue, probably due to its tight binding to the acidic residues in the acidic patch of the nucleosome. We then mapped the possible crosslinking areas for the H2A Lys95, H2B Lys120, and H3 Lys56 residues on the nucleosome structure, as colored circles with a 20-Å radius (Fig. 5b). The location of the ELYS Lys2400 residue was predicted in the area overlapped by these three circles (Fig. 5b). Interestingly, the predicted ELYS Lys2400 location overlaps with the extra density corresponding to part of ELYS_C in the cryo-EM structure (Fig. 5c). The ELYS Lys2400 residue exists near the ELYS RRK stretch (from 2404 to 2406), and the H2A Lys95, H2B Lys116, and H2B Lys120 residues are located near the acidic patch of the nucleosome. Therefore, the ELYS_C RRK stretch may directly bind to the acidic patch of the nucleosome.

The Lys residue that tightly bound to the acidic amino acid residue may not be crosslinked by DSS-H12/D12, because of steric hindrance. Therefore, the ELYS Lys2400 residue may be efficiently crosslinked with the Lys residues in the histone, because it may not tightly bind to the histone residues, although its localization must be very close to the RRK stretch.

Discussion

ELYS plays a key role in the post-mitotic NPC assembly mediated by nucleosomes^{16–18}. In fact, ELYS reportedly binds to the nucleosome in vitro and co-purified with histones in vivo^{23,24}. However, the mechanism of the ELYS–nucleosome binding has not yet been elucidated. In the present study, we reconstructed the structure of the ELYS_C-nucleosome complex by the cryo-EM method (Figs. 3 and 4). The cryo-EM structure, combined with the crosslinking mass spectrometry, demonstrated that the ELYS C-terminal region including the RRK stretch is important for binding to the acidic patch on the nucleosome surface (Figs. 3–5). Consistently, biochemical analyses revealed that the Arg and Lys residues in the ELYS RRK stretch function in the nucleosome binding (Figs. 1 and 2).

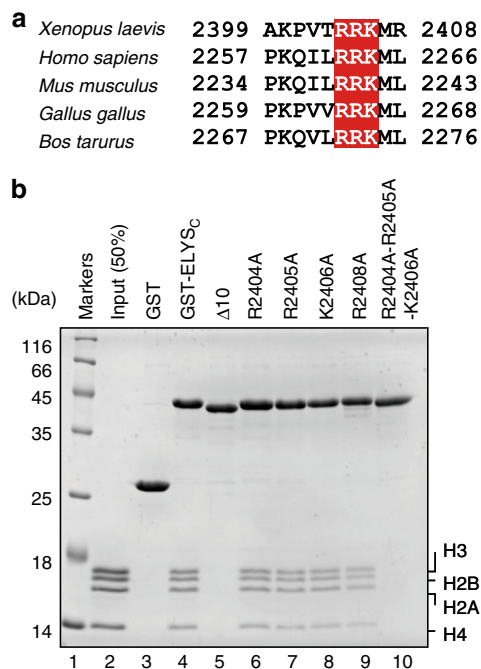


Fig. 2 The RRK stretch at the C-terminus of ELYS is important for nucleosome binding. **a** Sequence alignment of the *Xenopus laevis*, *Homo sapiens*, *Mus musculus*, *Gallus gallus*, and *Bos taurus* ELYS proteins. The RRK stretch is colored red. The amino acid residues are numbered. **b** The pull-down assay for the nucleosome with GST, GST-ELYS_C, or GST-ELYS_C mutants. Lane 1 represents molecular mass markers. Lane 2 indicates input nucleosome (50%). Lane 3 indicates a negative control experiment with GST. Lanes 4–10 represent the experiments with GST-ELYS_C and GST-ELYS_C mutants (R2404A, R2405A, K2406A, R2408A, and R2404A-R2405A-K2406A), respectively. Experiments were independently repeated three times, and consistent results were obtained. The uncropped gel image is shown in Supplementary Fig. 4

The RRK stretch containing Arg-Arg-Lys residues is highly conserved among ELYS orthologs (Fig. 2a). However, the functional importance of these residues has not been clarified. Here we found that the RRK stretch functions in binding to the nucleosomal acidic patch. The acidic patch comprises the H2A and H2B acidic amino acid residues, which are exposed on both sides of the nucleosome surface (Fig. 4). The acidic patches of the nucleosome provide binding sites for chromatin-associated factors, such as RCC1, Sir3, PRC1, CENP-C, and LANA^{29–33}. In these proteins, the arginine side chain specifically binds to the acidic patch on the nucleosome and is referred to as the arginine anchor²⁷. In the ELYS_C-nucleosome complex, the arginine residues in the RRK stretch of ELYS_C may also function as an arginine anchor. Our mutational analyses showed that all three basic residues, but not each residue, in the RRK stretch are required for the nucleosome binding (Fig. 2). Therefore, the binding mechanism of ELYS_C to the acidic patch of the nucleosome may be somewhat different from that of the conventional arginine anchor motif. Alternatively, one of the two arginine residues in the RRK stretch may redundantly function as an arginine anchor.

Consistent with previous results, our biochemical analyses revealed that the AT-hook region also functions in nucleosome binding (Fig. 1). Importantly, our mutational analyses demonstrated that the contribution of the RRK stretch may be higher than that of the AT-hook region in nucleosome binding (Fig. 1). In the ELYS_C-nucleosome complex structure, the AT-hook region was not visible, because of its flexible nature. The

AT-hook region of ELYS reportedly binds to DNA^{22,23}. The AT-hook motifs of other proteins reportedly prefer to bind to DNA-containing AT-rich regions²². Therefore, the DNA binding of the AT-hook region may support the ELYS nucleosome binding, which is mainly mediated by the binding of the RRK stretch to the acidic patch.

In vitro analyses revealed that importin β and transportin directly bind to the C-terminal region of ELYS (2359–2408) but not the AT-hook region³⁴. The importin β and transportin-binding region of ELYS contains the RRK stretch. Therefore, ELYS-nucleosome binding may compete with importin β and transportin binding and may inhibit ELYS recruitment to chromatin^{34,35}. Thus the release of ELYS from importin β and transportin may be a prerequisite for NPC assembly^{34,35}. RanGTP reportedly weakens the ELYS-importin β and ELYS-transportin interactions^{34,35}. Therefore, the RanGTP-mediated ELYS release from importin β and transportin may be important for the ELYS-chromatin association, which is the primary step for NPC assembly in the post-mitotic phase.

Methods

Purification of ELYS fragments and histones. Human histones H2A, H2B, H3.1, and H4 were produced in *Escherichia coli* cells^{36,37}. The denatured hexahistidine (His₆-tagged) human histone proteins were purified by chromatography using nickel-nitrilotriacetic acid (Ni-NTA) agarose beads (Qiagen). The His₆-tag portion was removed by thrombin protease treatment. After removal of the His₆-tag portion, the samples were further purified by chromatography using MonoS column (GE Healthcare). For the reconstitution of the histone octamer^{36,37}, four core histones (H2A, H2B, H3.1, and H4) were equally mixed in denaturing buffer (20 mM Tris-HCl (pH 7.5), 1 mM EDTA, 7 M guanidine hydrochloride, and 20 mM 2-mercaptoethanol). The reconstituted histone octamer was further purified by chromatography using Superdex 200 gel-filtration column (GE Healthcare).

The DNA fragment encoding *X. laevis* ELYS 2299–2408 (ELYS_C) was synthesized by the polymerase chain reaction (PCR) method. The amplified DNA fragment encoding ELYS_C was ligated into the *Nde*I site, which was artificially created by PCR mutagenesis in the pGEX-6p-1 vector. The GST-tagged ELYS_C protein was expressed in the *E. coli* BL21 (DE3) codon plus RIL strain (Stratagene). The cells were cultured at 30 °C, and the expression of GST-ELYS_C was induced when the cell growth reached an optical density of 0.6 (OD₆₀₀), by adding 0.5 mM IPTG and further culturing at 18 °C. The cells producing GST-ELYS_C were collected and resuspended in resuspension buffer 1, containing 50 mM Tris-HCl (pH 7.5), 500 mM NaCl, 1 mM EDTA, 10% glycerol, and 2 mM 2-mercaptoethanol. The cells were disrupted by sonication, and the supernatant was separated from the cell debris by centrifugation. The supernatant was gently mixed with Glutathione Sepharose 4B beads (GE Healthcare) at 4 °C for 1 h. The beads were packed into an Econo-column (Bio-Rad) and were washed with 50 column volumes of resuspension buffer 1. GST-ELYS_C was eluted by 30 column volumes of 50 mM Tris-HCl (pH 8.8) buffer, containing 500 mM NaCl, 1 mM EDTA, 20 mM reduced glutathione, and 2 mM 2-mercaptoethanol. The eluted sample was immediately applied to a HiLoad 16/60 Superdex 200 gel filtration column (GE Healthcare) equilibrated with 50 mM HEPES-NaOH (pH 7.5) buffer, containing 150 mM NaCl and 2 mM 2-mercaptoethanol. Aliquots of purified GST-ELYS_C were frozen in liquid nitrogen and stored at –80 °C. The GST-ELYS_C mutants (2R-A, Δ 10, R2404A, R2405A, K2406A, R2408A, and R2404A-R2405A-K2406A) were generated using a KOD-plus-mutagenesis Kit (TOYOBO), and the resulting ELYS_C mutants were purified by the same method as the wild-type ELYS_C purification.

For the purification of His₆-tagged ELYS_C, the N-terminally His₆-tagged ELYS_C protein was produced in the *E. coli* BL21 (DE3) codon plus RIL strain. The cells were cultured at 30 °C to an OD₆₀₀ = 0.6, and His₆-ELYS_C expression was induced by adding 0.2 mM IPTG and incubating the culture further at 18 °C. The cells producing His₆-ELYS_C were resuspended in resuspension buffer 2, containing 50 mM Tris-HCl (pH 8.0), 500 mM NaCl, 5 mM imidazole, 10% glycerol, and 2 mM 2-mercaptoethanol. The cell debris was removed by centrifugation. The supernatant was gently mixed with Ni-NTA agarose beads (Qiagen) at 4 °C for 1 h, and then the Ni-NTA beads were washed with 50 column volumes of resuspension buffer 2. The proteins bound to the Ni-NTA beads were eluted by a linear gradient of 5–500 mM imidazole. The fractions containing His₆-ELYS_C were collected, and the His₆-tag portion was removed by thrombin protease treatment (2 units/mg, GE Healthcare) during dialysis against 20 mM Tris-HCl (pH 7.5) buffer, containing 200 mM NaCl, 1 mM EDTA, 10% glycerol, and 2 mM 2-mercaptoethanol. After the His₆-tag portion was removed, the sample was loaded onto a MonoS column (GE Healthcare). The column was washed with 10 column volumes of 50 mM Tris-HCl (pH 8.0) buffer, containing 200 mM NaCl, 1 mM EDTA, 10% glycerol, and 2 mM 2-mercaptoethanol. The protein was eluted by a 30 column volume linear gradient of 200–900 mM NaCl. The peak fraction containing ELYS_C was immediately applied to a HiLoad 26/60 Superdex 75 gel filtration column (GE Healthcare) equilibrated with 20 mM HEPES-NaOH (pH 7.5) buffer, containing

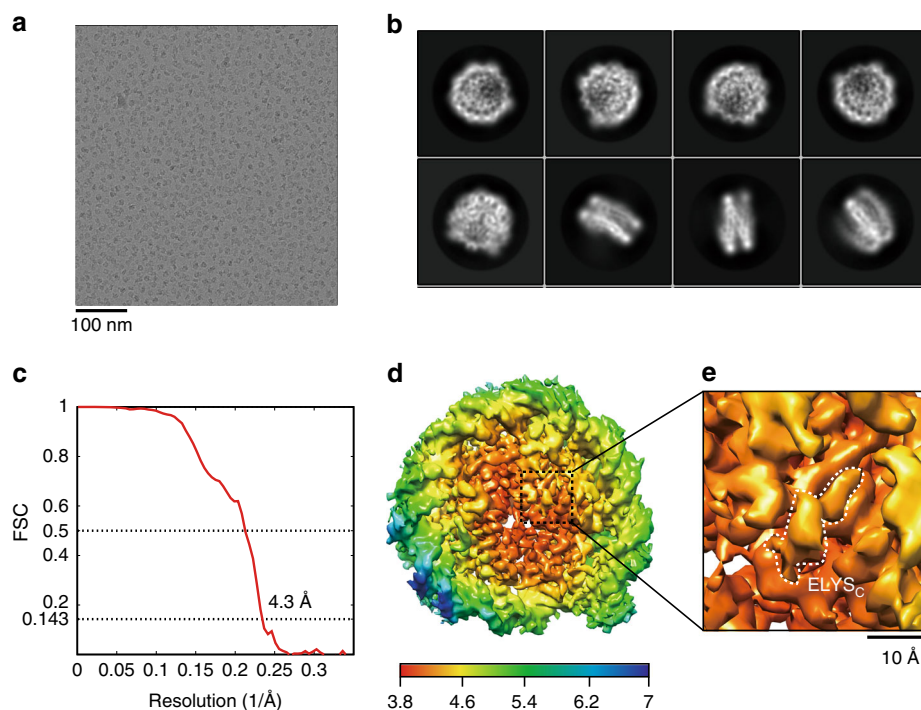


Fig. 3 The cryo-electron microscopic structure of the ELYS_C-nucleosome complex. **a** Digital micrograph of the ELYS_C-nucleosome complexes. Scale bar indicates 100 nm. **b** Selected two-dimensional class averages from single particle images of the ELYS_C-nucleosome complex. The box size is 21 nm². **c** Fourier shell correlation (FSC) curve after gold-standard map refinement. The overall resolution of the ELYS_C-nucleosome complex is 4.3 Å at an FSC = 0.143. **d** Local resolution map of the ELYS_C-nucleosome complex, showing the resolution range across the map from 3.8 to 7 Å. **e** Enlarged view of the ELYS density with a scale bar

Table 1 Cryo-EM data collection and image processing

Data collection and processing	ELYS _C -nucleosome (EMDB-9802)
Magnification	×100,000
Voltage (kV)	200
Electron exposure (e ⁻ /Å ²)	~56
Defocus range (μm)	-1.5 to -3.0
Pixel size (Å)	1.32
Symmetry imposed	C1
Initial particle images (no.)	1,300,821
Final particle images (no.)	81,008
Map resolution (Å)	4.3
FSC threshold	0.143
Accuracy of rotations (°)	1.904
Accuracy of translations (pix)	0.618
Map sharpening B factor (Å ²)	-218

Cryo-EM cryo-electron microscopy, FSC Fourier shell correlation

300 mM NaCl and 1 mM dithiothreitol (DTT). Aliquots of purified ELYS_C were frozen in liquid nitrogen and stored at -80 °C.

The concentrations of the ELYS_C and GST-tagged ELYS_C proteins were determined by sodium dodecyl sulfate-polyacrylamide gel electrophoresis (SDS-PAGE), with bovine serum albumin (BSA) as the standard protein.

Purification of nucleosomes. For the nucleosome reconstitution, the 145-bp DNA fragment containing the Widom 601 DNA was prepared^{38,39}. The nucleosomes were reconstituted by the salt dialysis method and prepared by polyacrylamide gel (6%) electrophoresis, using a Prep Cell apparatus (Bio-Rad). The nucleosomes were concentrated with an Amicon Ultra centrifugal filter unit (Millipore).

Gel-filtration analysis. ELYS_C and the nucleosome containing the 145-bp Widom 601 DNA were mixed in a 2.5:1 molar ratio in 10 mM Tris-HCl (pH 7.5) buffer, containing 35 mM NaCl and 1 mM DTT, at room temperature for 20 min. The reconstituted complex was subjected to chromatography on a Superdex 200 10/300 GL

gel filtration column (GE Healthcare) in 5 mM HEPES-NaOH (pH 7.5), 35 mM NaCl, and 2 mM TCEP.

The nucleosome pull-down assay. The nucleosome (1.1 μM) containing the 145-bp Widom 601 DNA was incubated with GST (2.5 μM), GST-ELYS_C (2.5 μM), or GST-ELYS_C mutants (2.5 μM of 2R-A, Δ10, R2404A, R2405A, R2406A, R2408A, and R2404A-R2405A-K2406A) at room temperature for 15 min in 20 μL of pull-down buffer (20 mM HEPES-NaOH (pH 7.5), 200 mM NaCl, 0.05% Triton-X, 0.5 mM TCEP, and 0.25 μg/mL BSA). Glutathione Sepharose 4B beads (15 μL) and pull-down buffer (500 μL) were added to the reaction mixtures, which were gently mixed at room temperature for 30 min. The beads were then washed three times with 1 mL of the pull-down buffer without BSA. The proteins that copelleted with the beads were denatured and were analyzed by 18% SDS-PAGE with Coomassie Brilliant Blue staining.

Preparation of the ELYS_C-nucleosome for cryo-EM analysis. GST-ELYS_C (12 μM) and the nucleosome containing the 145 bp Widom 601 DNA (4.8 μM) were mixed in a 2.5:1 molar ratio at room temperature for 20 min. The GST-ELYS_C-nucleosome complex was purified and stabilized by the Grafix method⁴⁰. A gradient was formed with buffer A (10 mM HEPES-NaOH (pH 7.5), 35 mM NaCl, 1 mM DTT, and 5% sucrose) and buffer B (buffer A with 20% sucrose and 4% paraformaldehyde), using a Gradient Master (BioComp). The reconstituted GST-ELYS_C-nucleosome complex (170 μL) was placed on the top of the gradient solution and was ultracentrifuged at 27,000 rpm at 4 °C for 16 h, using an SW32 Ti rotor (Beckman Coulter). One milliliter fractions were collected from the top of the gradient solution by pipetting and were analyzed by 6% non-denaturing PAGE. The collected samples were then desalted with a PD-10 column (GE Healthcare), equilibrated with 10 mM HEPES-NaOH (pH 7.5) buffer containing 2 mM TCEP and were concentrated with an Amicon Ultra centrifugal filter unit (Millipore). The DNA concentration of the sample was 432 μg/mL.

Cryo-EM specimen preparation and data acquisition. To prepare the cryo-EM specimen, the sample (2.5 μL) was applied to a glow-discharged holey carbon grid (Quantifoil R1.2/1.3 200-mesh Cu). The grids were blotted for 8.0 s under 100% humidity at 4 °C and were plunged into liquid ethane cooled by liquid nitrogen, using a Vitrobot Mark IV (Thermo Fisher). Images were collected using the EPU auto acquisition software on a Talos Arctica cryo-electron microscope (Thermo Fisher), operated at 200 kV, and equipped with a Quantum GIF filter (Gatan) in

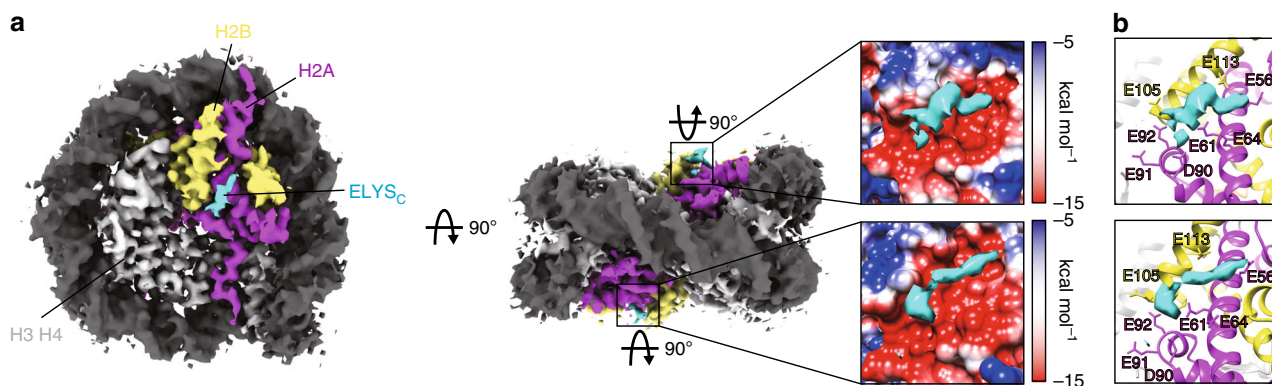


Fig. 4 ELYS_C interacts with the acidic patch of the nucleosome. **a** Cryo-electron microscopic structure of the ELYS_C-nucleosome complexes at 4.3 Å, contoured at 3.7 sigma above mean density. ELYS_C, H2A, and H2B are colored cyan, magenta, and yellow, respectively. Enlarged views around the acidic patches encircled with rectangles are presented. The acidic (red) and basic (blue) regions of the nucleosome surface are colored according to the Coulombic surface charge. The extra density corresponding to part of ELYS_C is colored cyan. **b** The acidic amino acid residues of the nucleosome surface around the ELYS_C region are presented. The H2A Glu56, Glu61, Glu64, Asp90, Glu91, and Glu92 residues are colored magenta. The H2B Glu105 and Glu113 residues are colored yellow

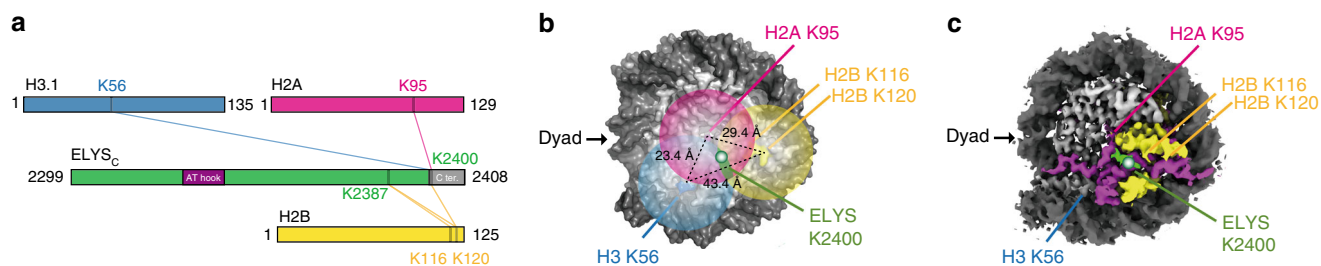


Fig. 5 The ELYS-nucleosome interaction determined by crosslinking mass spectrometry. **a** Schematic representation of the crosslinking mass spectrometric analysis. The interlinks between histone core regions (H2A, H2B, and H3.1) and ELYS_C are depicted with lines. The amino acid residues involved in the interlinks are indicated with numbers. The purple and gray boxes represent the regions corresponding to the AT-hook DNA-binding domain and the C-terminal ten amino acid residues, respectively. H3.1, H2A, H2B, and ELYS_C are colored blue, magenta, yellow, and green, respectively. **b** Possible location of the ELYS Lys2400 residue, predicted by the crosslinking mass spectrometric analysis. The black dashed lines with numbers show the distances between the C α atoms of the H2A Lys95, H2B Lys120, and H3 Lys56 residues. The red circle represents the 20 Å radius, which indicates the possible crosslinking area of the H2A Lys95 residue by DSS-H12/D12 (the central point is the C α atom). The yellow circle represents the 20 Å radius, which indicates the possible crosslinking area of the H2B Lys120 residue by DSS-H12/D12 (the central point is the C α atom). The blue circle represents the 20 Å radius, which indicates the possible crosslinking area of the H3.1 Lys56 residue by DSS-H12/D12 (the central point is the C α atom). The possible location of the ELYS Lys2400 residue is indicated as a green sphere. The crystal structure of the nucleosome containing a 145-bp Widom 601 DNA (PDB ID: 3IZ0) was used³⁹. The black arrow indicates the dyad axis of the nucleosome. **c** The cryo-electron microscopic structure of the ELYS_C-nucleosome complex. The predicted location of ELYS Lys2400 is superimposed on the structure

the energy-filtered transmission electron microscope mode, at a nominal magnification of $\times 100,000$ (pixel size of 1.32 Å). Images were recorded with 10-s exposure times on an energy-filtered (slit width 20 eV) K2 summit direct electron detector (Gatan) in the counting mode, retaining a total of 40 frames with a total dose of ~ 56 electrons/Å².

Image processing. In total, 2408 movies of the GST-ELYS_C-nucleosome complex were aligned and integrated using MOTIONCOR2⁴¹, with dose weighting. The contrast transfer function (CTF) was estimated by CTFIND4⁴² from the images, with dose weighting. In total, 1938 images were selected based on the CTF fit correlation to approximately 6 Å resolution. RELION 2.1⁴³ and RELION3.0 beta⁴⁴ were used for all subsequent image processing operations. In total, 1,300,821 particles of the GST-ELYS_C-nucleosome complex were picked automatically with a box size of 160 \times 160 pixels. Two rounds of two-dimensional classification to remove bad particles resulted in the selection of 868,748 particles. The ab initio model generated by RELION in the low-pass filter mode to 60 Å was used as the initial three-dimensional model. The class with GST density and the best resolution, containing 285,534 particles, was selected from the first round of three-dimensional classification, and 81,088 particles were further selected based on the CTF fit correlation to approximately 5.5 Å resolution before three-dimensional refinement. The final three-dimensional map was sharpened with an exponential B-factor (-218 Å²). The resolution of the refined map was estimated by the gold standard Fourier shell correlation (FSC) at the FSC = 0.143 criterion⁴³. The final

three-dimensional map was normalized with MAPMAN⁴⁵ and was mirrored to match the known handedness of the nucleosome. The local resolution map of the GST-ELYS_C-nucleosome complex was calculated with RELION⁴³. The iso-electron potential surface of the GST-ELYS_C-nucleosome complex was visualized with UCSF ChimeraX⁴⁶.

Crosslinking mass spectrometry. ELYS_C (11 μ M) was mixed with the nucleosome (4.4 μ M) containing the 145-bp Widom 601 DNA in a 2.5:1 molar ratio in 10 mM HEPES-NaOH (pH 7.5) buffer, containing 35 mM NaCl and 1 mM DTT, at room temperature for 20 min. After incubation, the sample was crosslinked with 240 μ M DSS-H12/D12 (Creative Molecules) at 30 °C for 30 min. The reaction was quenched by the addition of 100 mM ammonium bicarbonate and incubated at 30 °C for 15 min. The crosslinked peptides were prepared for the mass spectrometric analysis^{47–50}. The sample was evaporated to dryness and re-dissolved in an 8 M urea solution to a final concentration of 1 mg/mL. The crosslinked proteins were reduced by an incubation with 2.5 mM TCEP for 30 min at 37 °C and were alkylated by a further incubation with 5 mM iodoacetamide for 30 min at room temperature, with protection from light. The sample was diluted with a solution containing 50 mM ammonium bicarbonate to a final concentration of 1 M urea and digested with sequencing-grade endopeptidase Lys-C (Roche) at 37 °C for 2 h (at an enzyme-substrate ratio of 1:50 wt/wt), followed by a second digestion with Trypsin Gold, Mass Spectrometry Grade (Promega), at 37 °C overnight (at a 1:50 ratio wt/wt). The digestion was stopped by the addition of 5% (vol/vol) trifluoroacetic acid (TFA). All peptide samples were purified using

C18 spin columns (Pierce) eluted with 50% acetonitrile. The eluted sample was evaporated to dryness and was re-dissolved in water/acetonitrile/TFA, 75:25:0.1. Aliquots (30 μ L) of the crosslinked peptides were applied to a Superdex30 Increase 3.2/300 column (GE Healthcare), at a flow rate of 50 μ L/min with water/acetonitrile/TFA, 75:25:0.1. Fractions (100 μ L) were collected, dried, re-dissolved in 0.1% TFA, and subjected to the liquid chromatography tandem mass spectrometry (LC/MS-MS) analysis. LC/MS-MS analysis was conducted with an LTQ-Orbitrap Velos mass spectrometer (Thermo Fisher Scientific) equipped with a Zaplous Advance nano UHPLC HTS-PAL xt System (AMR). A fully porous particle C18 column (pore size 120 \AA , particle size 3 μ m, inner diameter 100 μ m, length 150 mm) was used for the nano LC, and the gradient, consisting of a linear gradient of the mobile phase developed from 5 to 50% of acetonitrile, was delivered at 300 nL/min over 90 min. The precursor ion was acquired over the mass range of 350–1500 Da, with a resolution of 60,000 full width at half maximum. In the data-dependent scan, single and unassigned charge precursors were rejected, and the ten most intense precursor ions were selected for MS/MS scans. The selected ions were sequentially isolated and fragmented in the linear ion trap by collision-induced dissociation. The crosslinked peptides were identified using xQuest, and the false-discovery rates (FDRs) were estimated by using xProphet⁴⁹. The results were filtered according to the following parameters: FDR < 0.05, minimum δ score = 0.85, MS1 tolerance window of -4 -4 ppm, ld-score > 25. The crosslinks were visualized using the webserver xVis⁵¹.

Reporting summary. Further information on experimental design is available in the Nature Research Reporting Summary linked to this article.

Data availability

The cryo-EM maps of the ELYS_C-nucleosomes have been deposited in the Electron Microscopy Data Bank, with the EMD ID code EMD-9802.

Received: 19 December 2018 Accepted: 8 March 2019

Published online: 03 May 2019

References

- Wolffe, A. P. *Chromatin: Structure & Function* (Academic Press, London, UK, 1998).
- Luger, K., Mäder, A. W., Richmond, R. K., Sargent, D. F. & Richmond, T. J. Crystal structure of the nucleosome core particle at 2.8 \AA resolution. *Nature* **389**, 251–260 (1997).
- Tan, S. & Davey, C. A. Nucleosome structural studies. *Curr. Opin. Struct. Biol.* **21**, 128–136 (2011).
- Koyama, M. & Kurumizaka, H. Structural diversity of the nucleosome. *J. Biochem.* **163**, 85–95 (2018).
- Paweletz, N. Walther Flemming: pioneer of mitosis research. *Nat. Rev. Mol. Cell Biol.* **2**, 72–75 (2001).
- Schellhaus, A. K., De Magistris, P. & Antonin, W. Nuclear reformation at the end of mitosis. *J. Mol. Biol.* **22**, 1962–1985 (2016).
- Macara, I. G. Transport into and out of the nucleus. *Microbiol. Mol. Biol. Rev.* **65**, 570–594 (2001).
- Pemberton, L. F. & Paschal, B. M. Mechanisms of receptor-mediated nuclear import and nuclear export. *Traffic* **6**, 187–198 (2005).
- Wente, S. R. & Rout, M. P. The nuclear pore complex and nuclear transport. *Cold Spring Harb. Perspect. Biol.* **2**, a000562 (2010).
- Hetzer, M., Walther, T. C. & Mattaj, I. W. Pushing the envelope: structure, function, and dynamics of the nuclear periphery. *Annu. Rev. Cell Dev. Biol.* **21**, 347–380 (2005).
- Güttinger, S., Laurrell, E. & Kutay, U. Orchestrating nuclear envelope disassembly and reassembly during mitosis. *Nat. Rev. Mol. Cell Biol.* **10**, 178–191 (2009).
- Smoyer, C. J. & Jaspersen, S. L. Breaking down the wall: the nuclear envelope during mitosis. *Curr. Opin. Cell Biol.* **26**, 1–9 (2014).
- Antonin, W., Ellenberg, J. & Dultz, E. Nuclear pore complex assembly through the cell cycle: regulation and membrane organization. *FEBS Lett.* **582**, 2004–2016 (2008).
- Weberuss, M. & Antonin, W. Perforating the nuclear boundary - how nuclear pore complexes assemble. *J. Cell Sci.* **129**, 4439–4447 (2016).
- Otsuka, S. & Ellenberg, J. Mechanisms of nuclear pore complex assembly - two different ways of building one molecular machine. *FEBS Lett.* **592**, 475–488 (2018).
- Rasala, B. A., Orjalo, A. V., Shen, Z., Briggs, S. & Forbes, D. J. ELYS is a dual nucleoporin/kinetochore protein required for nuclear pore assembly and proper cell division. *Proc. Natl Acad. Sci. USA* **103**, 17801–17806 (2006).
- Franz, C. et al. MEL-28/ELYS is required for the recruitment of nucleoporins to chromatin and postmitotic nuclear pore complex assembly. *EMBO Rep.* **8**, 165–172 (2007).
- Gillespie, P. J., Khoudoli, G. A., Stewart, G., Swedlow, J. R. & Blow, J. J. ELYS/MEL-28 chromatin association coordinates nuclear pore complex assembly and replication licensing. *Curr. Biol.* **17**, 1657–1662 (2007).
- Fernandez, A. G. & Piano, F. MEL-28 is downstream of the Ran cycle and is required for nuclear-envelope function and chromatin maintenance. *Curr. Biol.* **16**, 1757–1763 (2006).
- Galy, V., Askjaer, P., Franz, C., Lopez-Iglesias, C. & Mattaj, I. W. MEL-28, a novel nuclear-envelope and kinetochore protein essential for zygotic nuclear-envelope assembly in *C. elegans*. *Curr. Biol.* **16**, 1748–1756 (2006).
- Zierhut, C. & Funabiki, H. Nucleosome functions in spindle assembly and nuclear envelope formation. *Bioessays* **37**, 1074–1085 (2015).
- Rasala, B. A., Ramos, C., Harel, A. & Forbes, D. J. Capture of AT-rich chromatin by ELYS recruits POM121 and NDC1 to initiate nuclear pore assembly. *Mol. Biol. Cell* **19**, 3982–3996 (2008).
- Zierhut, C., Jenness, C., Kimura, H. & Funabiki, H. Nucleosomal regulation of chromatin composition and nuclear assembly revealed by histone depletion. *Nat. Struct. Mol. Biol.* **21**, 617–625 (2014).
- Inoue, A. & Zhang, Y. Nucleosome assembly is required for nuclear pore complex assembly in mouse zygotes. *Nat. Struct. Mol. Biol.* **21**, 609–616 (2014).
- Bilokapic, S. & Schwartz, T. U. Structural and functional studies of the 252 kDa nucleoporin ELYS reveal distinct roles for its three tethered domains. *Structure* **21**, 572–580 (2013).
- Gómez-Saldivar, G. et al. Identification of conserved MEL-28/ELYS domains with essential roles in nuclear assembly and chromosome segregation. *PLoS Genet.* **12**, e1006131 (2016).
- McGinty, R. K. & Tan, S. Recognition of the nucleosome by chromatin factors and enzymes. *Curr. Opin. Struct. Biol.* **37**, 54–56 (2016).
- Merkley, E. D. et al. Distance restraints from crosslinking mass spectrometry: mining a molecular dynamics simulation database to evaluate lysine-lysine distances. *Protein Sci.* **23**, 747–759 (2014).
- Makde, R. D., England, J. R., Yennawar, H. P. & Tan, S. Structure of RCC1 chromatin factor bound to the nucleosome core particle. *Nature* **467**, 562–566 (2010).
- Armache, K. J., Garlick, J. D., Canzio, D., Narlikar, G. J. & Kingston, R. E. Structural basis of silencing: Sir3 BAH domain in complex with a nucleosome at 3.0 \AA resolution. *Science* **334**, 977–982 (2011).
- McGinty, R. K., Henrici, R. C. & Tan, S. Crystal structure of the PRCl ubiquitylation module bound to the nucleosome. *Nature* **514**, 591–596 (2014).
- Kato, H. et al. A conserved mechanism for centromeric nucleosome recognition by centromere protein CENP-C. *Science* **340**, 1110–1113 (2013).
- Barbera, A. J. et al. The nucleosomal surface as a docking station for Kaposi's sarcoma herpesvirus LANA. *Science* **311**, 856–861 (2006).
- Lau, C. K. et al. Transportin regulates major mitotic assembly events: from spindle to nuclear pore assembly. *Mol. Biol. Cell* **20**, 4043–4058 (2009).
- Rotem, A. et al. Importin beta regulates the seeding of chromatin with initiation sites for nuclear pore assembly. *Mol. Biol. Cell* **20**, 4031–4042 (2009).
- Tachiwana, H. et al. Structural basis of instability of the nucleosome containing a testis-specific histone variant, human H3T. *Proc. Natl Acad. Sci. USA* **107**, 10454–10459 (2010).
- Kujirai, T. et al. Methods for preparing nucleosomes containing histone variants. *Methods Mol. Biol.* **1832**, 3–20 (2018).
- Lowary, P. T. & Widom, J. New DNA sequence rules for high affinity binding to histone octamer and sequence-directed nucleosome positioning. *J. Mol. Biol.* **276**, 19–42 (1998).
- Vasudevan, D., Chua, E. Y. & Davey, C. A. Crystal structures of nucleosome core particles containing the '601' strong positioning sequence. *J. Mol. Biol.* **403**, 1–10 (2010).
- Kastner, B. et al. GraFix: sample preparation for single-particle electron cryomicroscopy. *Nat. Methods* **5**, 53–55 (2008).
- Zheng, S. Q. et al. MotionCor2: anisotropic correction of beam-induced motion for improved cryo-electron microscopy. *Nat. Methods* **14**, 331–332 (2017).
- Mindell, J. A. & Grigorieff, N. Accurate determination of local defocus and specimen tilt in electron microscopy. *J. Struct. Biol.* **142**, 334–347 (2003).
- Scheres, S. H. Processing of structurally heterogeneous Cryo-EM data in RELION. *Meth. Enzymol.* **579**, 125–157 (2016).
- Zivanov, J. et al. New tools for automated high-resolution cryo-EM structure determination in RELION-3. *Elife* **7**, e42166 (2018).
- Kleywegt, G. J. et al. The Uppsala electron-density server. *Acta Crystallogr. D Biol. Crystallogr.* **60**, 2240–2249 (2004).
- Goddard, T. D. et al. UCSF ChimeraX: meeting modern challenges in visualization and analysis. *Protein Sci.* **27**, 14–25 (2017).
- Jennebac, S., Herzog, F., Aebersold, R. & Cramer, P. Crosslinking-MS analysis reveals RNA polymerase I domain architecture and basis of rRNA cleavage. *Nucleic Acids Res.* **40**, 5591–5601 (2012).
- Leitner, A. et al. Expanding the chemical cross-linking toolbox by the use of multiple proteases and enrichment by size exclusion chromatography. *Mol. Cell. Proteomics* **11**(M111), 014126 (2012).

49. Leitner, A., Walzthoeni, T. & Aebersold, R. Lysine-specific chemical cross-linking of protein complexes and identification of cross-linking sites using LC-MS/MS and the xQuest/xProphet software pipeline. *Nat. Protoc.* **9**, 120–137 (2014).
50. Gallego, L. D. et al. Structural mechanism for the recognition and ubiquitination of a single nucleosome residue by Rad6-Bre1. *Proc. Natl Acad. Sci. USA* **113**, 10553–10558 (2016).
51. Grimm, M., Zimniak, T., Kahraman, A. & Herzog, F. xVis: a web server for the schematic visualization and interpretation of crosslink-derived spatial restraints. *Nucleic Acids Res.* **43**, W362–W369 (2015).

Acknowledgements

We are grateful to Ms. Y. Iikura for her assistance. We also thank Dr. M. Kikkawa for cryo-EM measurements. This work was supported in part by JSPS KAKENHI Grant Numbers JP18H05534 [to H.K.], JP17H01408 [to H.K.], and JP18K14626 [to W.K.]. This work was also partly supported by JST CREST Grant Number JPMJCR16G1 and the Platform Project for Supporting Drug Discovery and Life Science Research (BINDS) from AMED, under Grant Number JP18am0101076 [to H.K.] and JP18am0101115j0002 [to M. Kikkawa].

Author contributions

W.K., M.A. and H.I. performed sample preparation and biochemical analyses. Y.T. and W.K. collected the cryo-EM images and reconstructed the structure of the ELYS_C-nucleosome complex. W.K. and L.N. performed the crosslinking MS analysis. W.K. and H.K. conceived, designed, and supervised all of the work and wrote the paper. All the authors discussed the results and commented on the manuscript.

Additional information

Supplementary information accompanies this paper at <https://doi.org/10.1038/s42003-019-0385-7>.

Competing interests: The authors declare no competing interests.

Reprints and permission information is available online at <http://npg.nature.com/reprintsandpermissions/>

Publisher's note: Springer Nature remains neutral with regard to jurisdictional claims in published maps and institutional affiliations.



Open Access This article is licensed under a Creative Commons Attribution 4.0 International License, which permits use, sharing, adaptation, distribution and reproduction in any medium or format, as long as you give appropriate credit to the original author(s) and the source, provide a link to the Creative Commons license, and indicate if changes were made. The images or other third party material in this article are included in the article's Creative Commons license, unless indicated otherwise in a credit line to the material. If material is not included in the article's Creative Commons license and your intended use is not permitted by statutory regulation or exceeds the permitted use, you will need to obtain permission directly from the copyright holder. To view a copy of this license, visit <http://creativecommons.org/licenses/by/4.0/>.

© The Author(s) 2019